INTERNATIONAL JOURNAL OF HYDROGEN ENERGY 33 (2008) 2189–2199

Available at www.sciencedirect.com

ScienceDirect

journal homepage: www.elsevier.com/locate/he

Thermochemical two-step water-splitting reactor with internally circulating fluidized bed for thermal reduction of ferrite particles

N. Gokon[a,*], S. Takahashi[a], H. Yamamoto[a], T. Kodama[a,b]

[a]Graduate School of Science and Technology, Niigata University, 8050 Ikarashi 2-nocho, Nishi-ku, Niigata 950-2181, Japan
[b]Department of Chemistry and Chemical Engineering, Faculty of Engineering, Niigata University, 8050 Ikarashi 2-nocho, Nishi-ku, Niigata 950-2181, Japan

ARTICLE INFO

Article history:
Received 2 May 2007
Received in revised form
12 November 2007
Accepted 16 February 2008
Available online 7 April 2008

Keywords:
Iron oxides
Ferrites
Hydrogen
Solar
Reactor
Concentrated solar radiation
Water-splitting

ABSTRACT

A thermochemical two-step water-splitting cycle using a redox system of iron-based oxides or ferrites was examined on hydrogen productivity and reactivity of ferrite in order to convert solar energy into hydrogen in sunbelt regions. In the present paper, a new concept is proposed for a windowed thermochemical water-splitting reactor, using an internally circulating fluidized bed of $NiFe_2O_4/m$-ZrO_2 particles, and thermal reduction of the bed is demonstrated on a laboratory scale by using a solar-simulating Xe-beam irradiation. The concept is that concentrated solar radiation passes through the transparent window and directly heats the internally circulating fluidized bed. The fluidized bed reactor enabled the $NiFe_2O_4/m$-ZrO_2 sample to remain in powder form without sintering and agglomerating during direct Xe-beam irradiation over 30 min. Approximately 45% of the $NiFe_2O_4$ was converted to the reduced phase by the solar-simulated high-flux beam, and was then completely reoxidized with steam at 1000 °C to generate hydrogen.

1. Introduction

Modern solar concentration systems such as the central-tower and dish type systems can provide high-temperature solar thermal energy at levels up to hundreds of megawatts and a few hundred-kilowatts, respectively [1–3], when utilized in "sunbelt" regions that are greatly insolated, such as the southwest US, southern Europe, Australia, and broad regions of the developing world. The conversion of high-temperature solar heat to hydrogen has the advantage of producing long-term storable and transportable energy carriers from solar energy.

One promising solar thermochemical cycle is a two-step water-splitting cycle for hydrogen production from water using a metal-oxide redox pair. This process, originally proposed by Nakamura [4], is as follows:

$$Fe_3O_4 = 3FeO + \tfrac{1}{2}O_2, \quad \Delta H^{\circ}_{298\,K} = 319.5\,kJ\,mol^{-1} \quad \text{(Thermal-reduction step)}, \tag{1}$$

$$3FeO + H_2O = Fe_3O_4 + H_2, \quad \Delta H^{\circ}_{298\,K} = -33.6\,kJ\,mol^{-1} \quad \text{(Water-decomposition step)}. \tag{2}$$

This first high-temperature process is highly endothermic while the second process is slightly exothermic at moderate temperatures. The thermodynamic analysis indicates that the solar high-temperature step in the thermal reduction of Fe_3O_4 to FeO (Eq. (1)) proceeds at temperatures above 2500 K under a pressure of 1 bar [5]. The iron–oxygen phase diagram

*Corresponding author. Tel./fax: +81 25 262 7542.
E-mail address: ngokon@eng.niigata-u.ac.jp (N. Gokon).
0360-3199/$ - see front matter © 2008 International Association for Hydrogen Energy. Published by Elsevier Ltd. All rights reserved.
doi:10.1016/j.ijhydene.2008.02.044

by Darken and Gurry shows that Eq. (1) can proceed to some extent at 1300–1400 °C if it is performed under an oxygen partial pressure lower than 10^{-6} bar [6]. Solid solutions between the redox system Fe_3O_4/FeO and M_3O_4/MO (M = Mn and Co) have been examined with the possibility of combining the high H_2 yields from the Fe_3O_4/FeO system with the low-reduction temperature of a M_3O_4/MO system [7–10].

However, the Fe_3O_4/FeO redox pair is rapid deactivation of the iron oxide particles in the cyclic reaction. This is due to melting and sintering of iron oxide particles at high temperature. The present authors first demonstrated repeatable two-step water-splitting in 2003, using highly active "ZrO_2-supported" ferrite particles [11–13]. The supporting ZrO_2 alleviated agglomeration or sintering of the solid ferrite reactant, and as a result the cyclic reaction could be repeated with relatively good activity in the temperature range of 1000–1400 °C. In a recent study, ZrO_2-supported $NiFe_2O_4$ was found to show the highest hydrogen productivity (hydrogen production of 13.6 $Ncm^3\,g^{-1}$ material on an average), superior reactivity (ferrite conversion of 69% on an average), and repeatability for the two-step water-splitting cycle [13].

In order to realize the two-step water-splitting using concentrated solar radiation as the energy source, development of an appropriate chemical reactor system is required. The first endothermic step, thermal reduction of the redox material, requires a very high temperature of approximately 1300–1400 °C. Therefore, the redox material loaded in the chemical reactor must be directly irradiated by a high flux of concentrated solar radiation. With respect to this requirement, some solar reactor concepts that realize direct solar radiation have been proposed or demonstrated for two-step water-splitting by redox materials [14–18].

Recently, the use of multi-channeled honeycomb ceramic supports coated with an active redox material of Fe_3O_4 (or magnetite) powder was proposed for a solar receiver–reactor system, in a configuration similar to that encountered in automobile exhaust catalytic converters [14,15]. The magnetite-coated honeycombs are directly irradiated by concentrated solar radiation through a quartz window, and heated to 1200 °C to thermally reduce the coated redox magnetite, while passing N_2 gas through the magnetite-coated honeycomb support. A cluster of these honeycomb reactors is constructed on the top of a solar tower, which allows the reactor to be scaled up to the multi-megawatt scale [15].

Another reactor concept uses reactant particles fed into a rotating cavity reactor with a window [16]. In addition, the volumetric gas-particle solar receiver–reactor has been examined for more than a decade [17]. The reactor concept is based on direct solar irradiation of a "suspension" of reactant particles in a gas stream, providing efficient heat transfer directly to a large mass of reactant particles. Thus, one can expect this type of reactor to reveal greater hydrogen productivity than the other reactor types mentioned above. Provided that the reactor is combined with a conventional solar concentration system such as a solar tower, a high-solar flux must enter horizontally or vertically into the reactor housing through a window at the side of the reactor (Fig. 1(a)). A solar reactors of this type have been previously constructed and demonstrated using a gas-particle vortex flow confined to a solar cavity receiver with a window [18].

Solar chemical reactors, such as a solar reformer, have recently been proposed for combination with newly developed solar reflective towers or beam-down optics [19,20]. Beam-down optics have an advantage over the conventional tower top reactor arrangement, in that they allow a large-scale reactor to be built on the ground, and the solar radiation enters the reactor housing through a window in the ceiling of the reactor. In such a reactor design, fluidized beds of reactant particles can be applied, because an interspacing gap is created between the fluidized particle bed and the window to avoid contact, as shown in Fig. 1(b).

In this study, the concept of the water-splitting reactor is first proposed. On the basis of the reactor concept, windowed chemical reactors of quartz tube (first test reactor) and stainless steel tube (second test reactor) were constructed, and tested for the thermal reduction of $NiFe_2O_4/ZrO_2$ particles in an internally circulating fluidized bed at a laboratory scale by using a solar-simulating Xe-beam irradiation. These two different materials of quartz and stainless steel have heat resistance and toughness at high temperature, which is suitable for construction and performance test of the reactors by solar-simulator with a low-energy flux. If the reactors are tested for the thermal reduction of $NiFe_2O_4/ZrO_2$ by solar irradiation with a high-energy flux, the reactor may require the coating of inner wall of that with higher heat resistant material such as ZrO_2 and SiC than stainless steel.

1.1. *Concept of a solar reactor with an internally circulating fluidized bed of reactant particles*

Fig. 2 shows a schematic example of the prototype reactor using an internally circulating fluidized bed of reactant particles. The cylindrical reactor body is made of stainless steel with a transparent quartz window installed in the ceiling of the reactor. A draft tube is centrally inserted in the fluidized bed region. Gases are separately introduced into the draft tube and annulus regions in the bed. The concentrated solar radiation passes downwards through the window and directly heats the internally circulating fluidized bed of reactant particles. In this system, the particles are always transported upwards in the draft tube and move downwards in the annulus section. This particle circulation within the reactor provides solar energy transfer from the top of the fluidized bed to the bottom, because directly solar-heated particles in the top region always move to the bottom region. This creates a more uniform temperature distribution through the solar-irradiated fluidized bed, when compared with a conventional solar-irradiated fluidized bed. In addition, the reactor is equipped with a shutter for control of the solar input energy. In the case of cloud passage during a short period of time, the shutter is closed to circumvent the temperature lowering of the fluidized bed.

Previously, the thermally reduced reactant particles by using a fixed bed reactor have required that the reduced particles be pulverized by pestle and mortar [13]. In the case of a fluidized bed reactor, if the internally circulating fluidized bed of reactant particles does not cause sintering and agglomeration by direct solar irradiation during or after thermal reduction, then the pulverization process would not

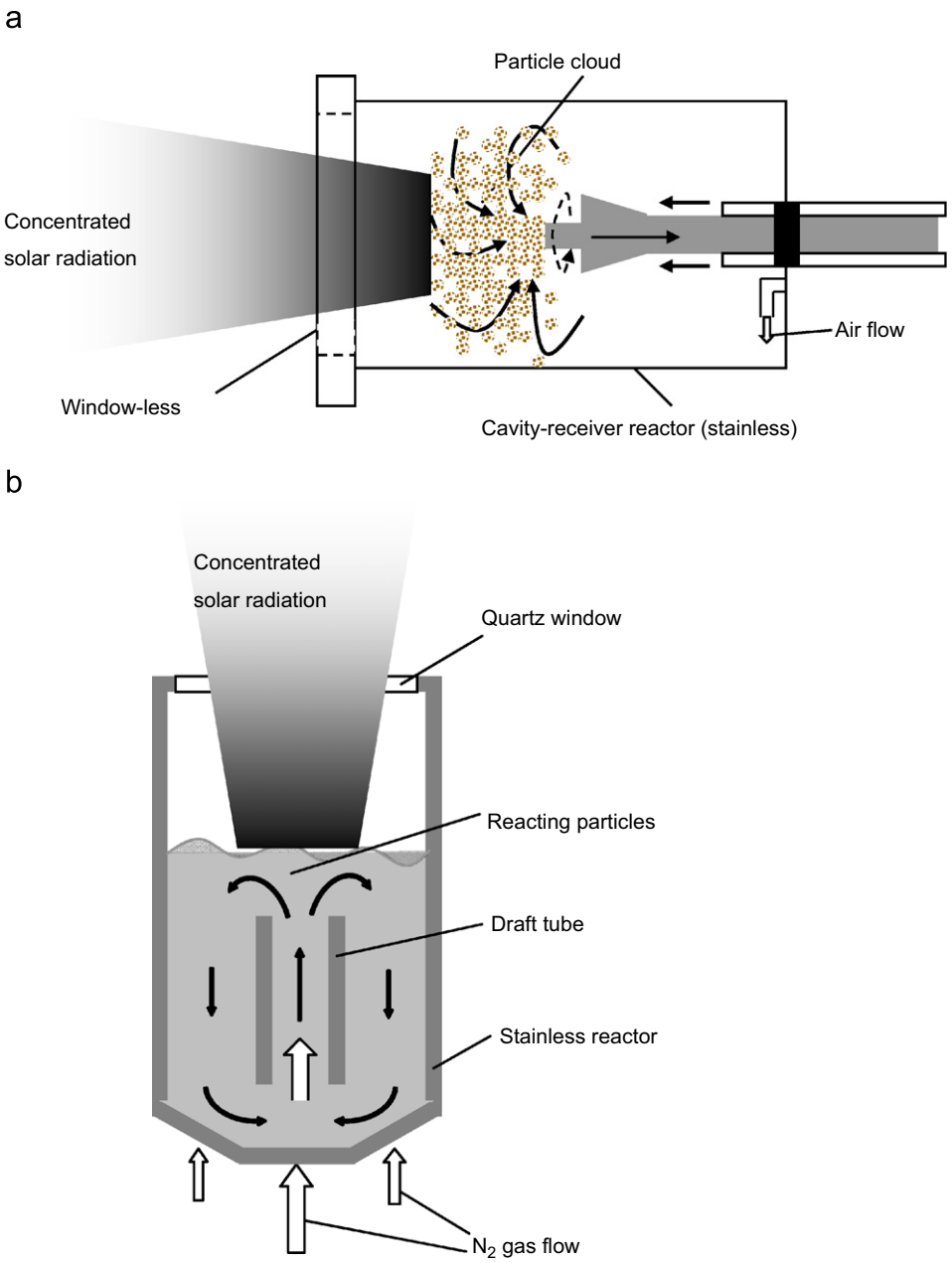

Fig. 1 – Schematics of: (a) a gas-particle solar receiver–reactor and (b) a fluidized bed reactor.

be required prior to the water-decomposition step. Therefore, in principle, the internally circulating fluidized bed reactor with reactant particles will be able to conduct the thermochemical two-step water-splitting cycle in a single reactor, by switching the feed gas between an inert gas (nitrogen) for the thermal-reduction step to steam for the water-decomposition step.

2. Experimental procedure

2.1. *Preparation of ZrO_2-supported $NiFe_2O_4$ powder*

ZrO_2-supported $NiFe_2O_4$ (Ni-ferrite/ZrO_2) powder was prepared by the coating of ZrO_2-support particles with $NiFe_2O_4$ using aerial oxidation of aqueous suspensions of Fe(II) hydroxide (the aerial Fe^{2+}-oxidation wet method) [11,13]. Ferrite can be directly plated on various substrate surfaces, such as organic compounds (Polyethylene terephthalate, Polymethylmethacrylate and Teflon), glass slides and metal (stainless steel), by insertion in an aqueous solution of Fe(II) sulfate; likewise, other bivalent M^{2+} ions (M = Mn, Mg, Ni, or Co, etc.) can be plated [21,22]. Hydrolyzed metal ions $FeOH^+$ and MOH^+ in the aqueous solution are adsorbed onto a substrate surface, and then react to form ferrite deposits associated with air oxidation of the $FeOH^+$ ions. Therefore, it was expected that $NiFe_2O_4$ could be deposited on the surface of the suspended ZrO_2-support particles using the aerial Fe^{2+}-oxidation wet method. Monoclinic ZrO_2 particles with 98% purity were used as the support. The size of the ZrO_2

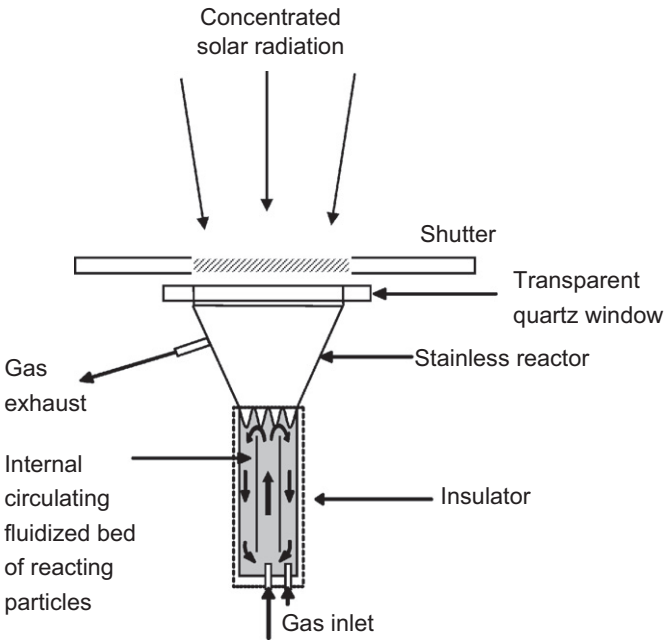

Fig. 2 – Schematic illustration of the prototype reactor, using an internally circulating fluidized bed of reactant particles.

particles was ca. 1 μm, and the Brunauer–Emmett–Teller (BET) surface area was measured to be 12.6 $m^2 g^{-1}$ (SHIMADZU, TriStar3000). The ZrO_2 powder was previously suspended in oxygen- and CO_2-free distilled water. After passing N_2 for a few hours, appropriate amounts of $NiSO_4$ and $FeSO_4$ were dissolved in the solution containing the ZrO_2 suspension. The solution was adjusted to a pH of 8–9 by adding 0.15 mol dm^{-3} NaOH solution to form $Ni(OH)_2$ and $Fe(OH)_2$. The content of $NiFe_2O_4$ in $NiFe_2O_4/ZrO_2$ was set to be ca. 20% by weight. After heating to 65 °C, air was bubbled through the suspension, while maintaining a pH of 8–9 by adding 0.15 mol dm^{-3} NaOH solution. The product was collected by centrifuging at 4000 rpm. After washing with distilled water and then with acetone, the product was dried *in vacuo* at 60 °C for one day. The powder was then calcined at 900 °C in an N_2 atmosphere before using in the high-temperature reactions.

Samples were identified using X-ray diffractometry (XRD) with CuK_α radiation (MAC Science, MX-Labo). XRD patterns of the $NiFe_2O_4/ZrO_2$ sample revealed only small peaks due to spinel ferrite along with strong peaks of the monoclinic ZrO_2 support.

To determine the chemical composition of the ferrite phase, the $NiFe_2O_4$ component of the ZrO_2-supported $NiFe_2O_4$ was dissolved in HCl solution and the solution was analyzed for Fe and Ni content using inductively coupled plasma-atomic emission spectrometry (ICP-AES; Seiko Instruments SPS-1500V). The ferrite content in the $NiFe_2O_4/m$-ZrO_2 used was 19.6% by weight.

2.2. *Setup and testing of the solar water-splitting reactor*

As a first reactor for testing the thermal reduction of $NiFe_2O_4/ZrO_2$ particles, an internally circulating fluidized bed reactor was constructed using quartz tubes, as illustrated in Fig. 3(a). The diameter of the outer tube is 45 mm (inside diameter 40 mm) and the thickness is 2.5 mm. The diameter of the inner centrally located draft tube was 20 mm with 2.5 mm thickness, and the tube length was 10 mm. The bottom of the draft tube was positioned 11 mm above the porous quartz frit of the distributor. In addition, a conical-shaped quartz cap tube (the inside diameter of the top was 6 mm and that of the bottom was 11 mm) (Fig. 3(b)) was fixed on the distributor to increase the carrier gas flow in the draft tube compared with that in the outer annular section. Carrier gas was allowed to flow upwards through the tubes to create the internal circulating fluidized bed of $NiFe_2O_4/ZrO_2$ particles. An amount of 20–40 g of $NiFe_2O_4/ZrO_2$ particles were loaded into the reactor. The static bed height was varied from 20 to 40 mm depending on the mass of loaded reactant particles.

This reactor was placed below a 6 kW Xe-arc lamp to simulate the sun (Nihon Koki, UXL-6000H) with the central axis of the reactor aligned with the axis of the oval concentrator of the sun-simulator (Figs. 3 and 4). The concentrator of the sun-simulator reflected the Xe-lamp beam downwards to the focal spot. The top of the static bed was set on the focal spot and the focal diameter of the spot was varied from 4 to 5 cm. The intensity and distribution of the concentrated Xe-lamp beam on the spot could be varied by changing the power supply to the Xe-arc lamp or by changing the focal diameter of the spot. The energy flux density of the Xe-lamp beam spot was previously measured using a heat flux transducer with a sapphire window attachment (Medtherm, 64-100-20/SW-1C150).

A N_2 gas stream (99.999%) was introduced as a carrier gas from the bottom of the reactor to create the internal circulating fluidized bed. The reactor was preheated at 900 °C using a cylindrical electric furnace. The preheater was controlled using a R-type thermocouple in contact with the exterior reactor wall. While passing the N_2 gas stream at a flow rate of 1.0−5.0 $Ndm^3 min^{-1}$, the internally circulating fluidized bed was directly irradiated and heated with the

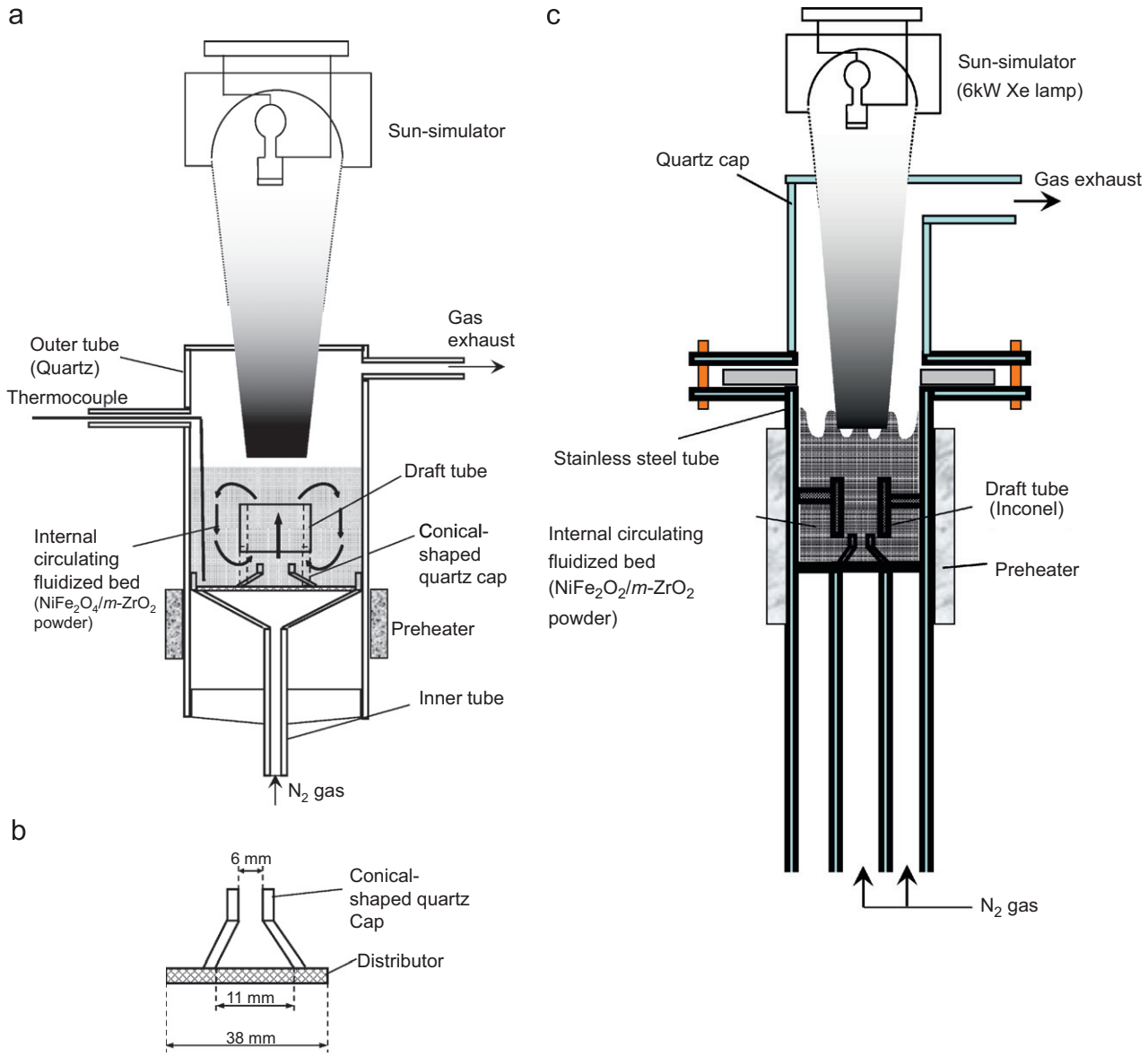

Fig. 3 – Experimental setup for the thermal-reduction (T-R) step using: (a) an internally circulating fluidized bed quartz reactor with draft tube, (b) a conical-shaped cap and (c) an internally circulating fluidized bed stainless steel reactor with draft tube.

concentrated Xe-lamp beam. This process will be referred to as the thermal-reduction (T-R) step. The bed temperature at the bottom of the annular section was measured using a K-type thermocouple inserted into the reactor.

Following irradiation, the fluidized bed was cooled to room temperature. The solid samples were then analyzed using XRD. In order to assess possible sintering or agglomeration of the supported particles, the BET surface area was measured and compared with the previous results of thermally reduced $NiFe_2O_4/ZrO_2$ particles at 1400 °C by a fixed bed reactor.

A portion of the thermally reduced $NiFe_2O_4/ZrO_2$ powder (ca. 1 g) was taken from the reactor, and pulverized using a pestle and mortar. The reason why this pulverization was performed is to compare a thermal reduction of $NiFe_2O_4/ZrO_2$ by a fluidized bed reactor with that so far obtained by a fixed bed reactor [13]. The pulverized solid sample was packed in another quartz tube fixed bed reactor with an inner diameter of 7 mm (Fig. 5) in order to perform the water-decomposition (W-D) step. A H_2O/N_2 gas mixture, produced by passing N_2 gas at a flow rate of 4×10^{-3} $Ndm^3\,min^{-1}$ through distilled water at 80 °C, was introduced into the reactor. The partial pressure of steam in the H_2O/N_2 mixture was estimated to be 47% from the steam vapor pressure at 80 °C and at 1 atm. The reactor was heated to 1000 °C within 10 min using an infrared furnace (Ulvac-Riko, RHL-E45P). The temperature was controlled using a K-type thermocouple in contact with the sample bed located inside the reactor. The W-D step was performed at 1000 °C for 60 min. To determine the volume of hydrogen evolved during the W-D step, the effluent was collected in a bottle by the water-displacement method. After the W-D step, the volume of collected effluent was measured and the gas composition was determined by gas chromatography (GC; Shimadzu, GC-4C) using a thermal conductivity detector (TCD).

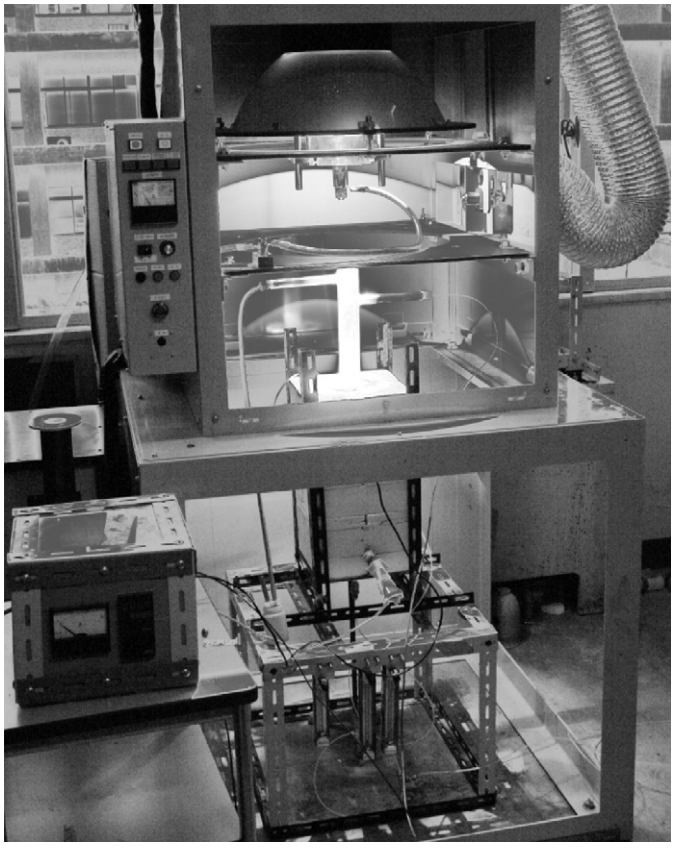

Fig. 4 – Photograph of the internal circulating fluidized bed reactor placed below the sun-simulator.

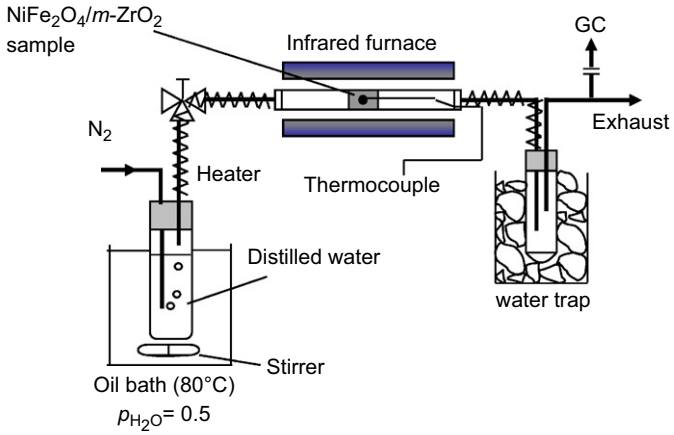

Fig. 5 – Experimental setup for the water-decomposition (W-D) step using the quartz tube reactor with a fixed bed.

A second internally circulating fluidized bed reactor for testing the thermal reduction of $NiFe_2O_4/ZrO_2$ particles was constructed using stainless steel tubes, and is schematically illustrated in Fig. 3(c). The inside diameter of the outer stainless steel tube was 45 mm with a thickness of 2.5 mm. The internal centrally located draft tube of the reactor was made of Inconel, with an inner diameter of 17 and 2 mm thickness, and a length of 20 mm. The bottom of the draft tube was positioned 12 mm above the porous stainless steel frit of the distributor. In addition, a conical-shaped stainless steel cap tube (the inside diameter of the top was 6 mm and that of the bottom was 18 mm) was fixed on the distributor. The N_2 carrier gas was allowed to flow upwards through the tubes to create the internal circulating fluidized bed of ZrO_2-supported $NiFe_2O_4$ particles. An amount of 35 g of the $NiFe_2O_4/ZrO_2$ particles was loaded into the reactor. The sun-simulating beam irradiation for thermal reduction was performed in the same manner as for the quartz reactor. The subsequent W-D step was performed by using the fixed bed reactor shown in Fig. 5.

The conversion of ferrite to the reduced wustite ($Fe_yNi_{1-y}O$) phase on the monoclinic ZrO_2 support was estimated from the volume of hydrogen produced by assuming that the wustite phase formed in the T-R step was completely reoxidized to ferrite in the subsequent W-D step.

Energy conversion η of a reactor was estimated from the volume of oxygen produced by assuming that the volume of oxygen evolved in the T-R step was a half volume of hydrogen production in the W-D step. The energy conversion of the reactor was defined as the fraction of incident Xe-beam power input entering through the reactor's aperture that is absorbed as enthalpy change of thermal reduction of $NiFe_2O_4$:

$$\eta = \frac{\Delta H}{Q_{Heat}}, \tag{3}$$

where Q_{Heat} is Xe-beam input energy of concentrated Xe-beam irradiation into a reactor, and ΔH is enthalpy change of thermal reduction of $NiFe_2O_4$.

3. Results and discussion

Fig. 6 shows a tentative profile for the energy flux density of the incident solar-simulated Xe-beam on the irradiated surface of the bed. The central peak of flux density reached 1110 kW m^{-2}. The input power of the incident Xe-beam was 0.82 kW. Almost all of the high-energy flux entered the reactor and directly irradiated the fluidized bed.

In order to compare the internal circulating fluidized bed design (Fig. 3 (a)) for a reactor without a draft tube (conventional fluidized bed reactor), thermal reduction of the $NiFe_2O_4/ZrO_2$ sample was performed using a quartz tube reactor without a draft tube. This reactor was initially loaded with 22 g of $NiFe_2O_4/ZrO_2$, to simulate a conventional fluidized bed of $NiFe_2O_4/ZrO_2$ particles. Fig. 7 shows the volume of hydrogen production and ferrite conversion as a function of time, estimated from the volume of hydrogen produced in the

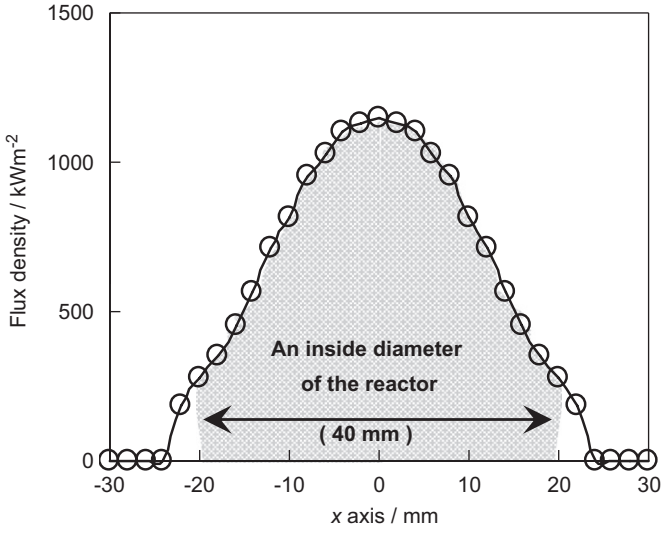

Fig. 6 – Flux density profile of the Xe beam irradiation. The input energy of the incident Xe-beam into the reactor was estimated by integrating the profile (gray area in the profile). The maximum energy flux density is the power density of the incident beam at the central position of the spot.

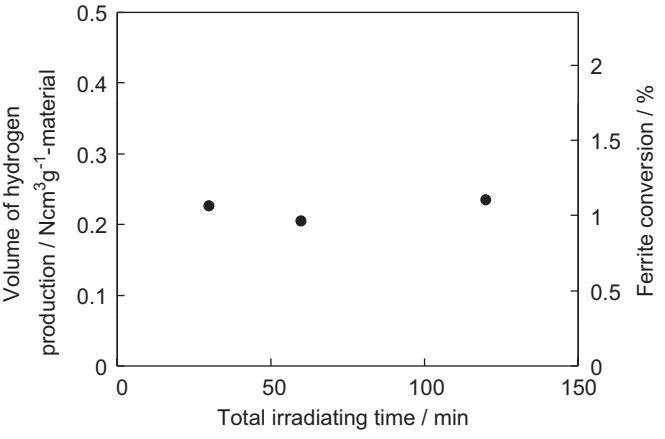

Fig. 7 – Hydrogen production and estimated ferrite conversion in the conventional quartz tube fluidized bed reactor as a function of irradiation time.

subsequent W–D step, for the conventional fluidized bed reactor (quartz tube). The volume of hydrogen produced was approximately 0.20 Ncm^3 per weight of material (including both $NiFe_2O_4$ and ZrO_2), and the ferrite conversion was only approximately 1%, although the irradiation time was increased to 120 min in the T-R step. The bed temperature at the bottom of the annular section was 900−1000 °C during the T-R step of Xe-beam irradiation.

A draft tube made of quartz tube was installed in the above-mentioned conventional fluidized bed reactor, and tested as a first chemical reactor for thermal reduction of the $NiFe_2O_4/ZrO_2$ (Fig. 3 (a)). Firstly, the thermal reduction of the $NiFe_2O_4/m$-ZrO_2 sample was performed under the same sample weight and irradiation conditions (1st run in Table 1) to compare with the conventional fluidized bed reactor described above. When the internally circulating fluidized bed of sample was irradiated for 60 min (1st run in Table 1), the hydrogen production and the estimated ferrite conversion significantly increased to 3.4 Ncm^3 per weight of material and 15%, respectively. In this case, the bed temperature was 1000−1200 °C at the bottom of the annular section during the irradiation. These results suggest that the internal circulation of the $NiFe_2O_4/m$-ZrO_2 particles effectively enhances the heat transfer from the top of the bed to the bottom by the draft tube installed inside the reactor. After the 1st run, the sample weight was doubled (ca. 40 g total), and then the sample was irradiated for 120 and 240 min under the same irradiation conditions (2nd and 3rd runs in Table 1). As a result, the volume of hydrogen produced and the ferrite conversion were decreased to approximately half of that for the 1st run. In addition, similar levels of activity for hydrolysis were obtained for both irradiation periods of 120 and 240 min. This implies that this reactor does not require such a long irradiation time for thermal reduction. Therefore, there is a possibility to further shorten the irradiation time for thermal reduction of the particle bed.

A further series of experiments were conducted, where the intensity of the irradiating Xe-beam flux was increased in order to improve the ferrite conversion of the $NiFe_2O_4/ZrO_2$ sample. The experimental conditions and the results are given in Table 2. In this series of experiments, 35 g of newly prepared $NiFe_2O_4/ZrO_2$ particles were tested in the reactor. The volume of hydrogen produced per weight of material was >4 times in comparison with the previous case (2nd and 3rd runs of Table 1), and the estimated ferrite conversion in the T-R step reached 29%. After further irradiation of 30 min (total irradiation time 60 min), as given in Table 2, the ferrite conversion of the powder sample increased to 45% (2nd run of Table 2). When the total irradiation time was doubled, the ferrite conversion did not double, but was increased by approximately 1.6 times. This indicates that the particle size of the fluidized $NiFe_2O_4/ZrO_2$ sample increased during the thermal reduction, resulting in decreasing the reaction rate for thermal reduction of the fluidized $NiFe_2O_4/ZrO_2$ sample.

Fig. 8 shows the changes of the XRD patterns for the $NiFe_2O_4/ZrO_2$ sample when the ferrite conversion reached 45%. After the T-R step, the reflection peaks due to $NiFe_2O_4$ become less intense. In addition, a small peak of the reflection due to Ni-doped wustite ($Fe_yNi_{1-y}O$) appears along with strong peaks of the monoclinic ZrO_2 support (Fig. 8 (a) and (b)). The Ni-doped wustite peak disappeared after the W-D step (Fig. 8 (c)) and the spinel Ni-ferrite peaks increased

Table 1 – Hydrogen production volume and ferrite conversion by a quartz reactor with the internally circulating fluidized bed

Run times	Sample weight (g)	Irradiation time (min)	Input energy (kW)	Peak flux density ($kW\,m^{-2}$)	Volume of hydeogen ($Ncm^3\,g^{-1}$ material)	Ferrite conversion (%)
1st	21.5	60	0.82[a]	1110[b]	3.4	15.3
2nd	40.3	120	0.82[a]	1110[b]	1.5	6.6
3rd	38.7	240	0.82[a]	1110[b]	1.4	6.4

[a] Input power of the incident Xe-beam into the reactor.
[b] Maximum energy flux density of the incident beam at the central position of the spot.

Table 2 – Hydrogen production volume by the internal circulating $NiFe_2O_4/ZrO_2$ fluidized bed reactor of quartz tube

Total irradiating time (min)	Sample weight (g)	Input energy (kW)	Volume of hydrogen ($Ncm^3\,g^{-1}$ material)	Ferrite conversion (%)
30	35	1.18 ($2964\,kW/m^2$)[a]	6.0	29
60	35	1.18 ($2964\,kW/m^2$)[a]	9.5	45

[a] Maximum energy flux density of the incident beam at the central position of the spot.

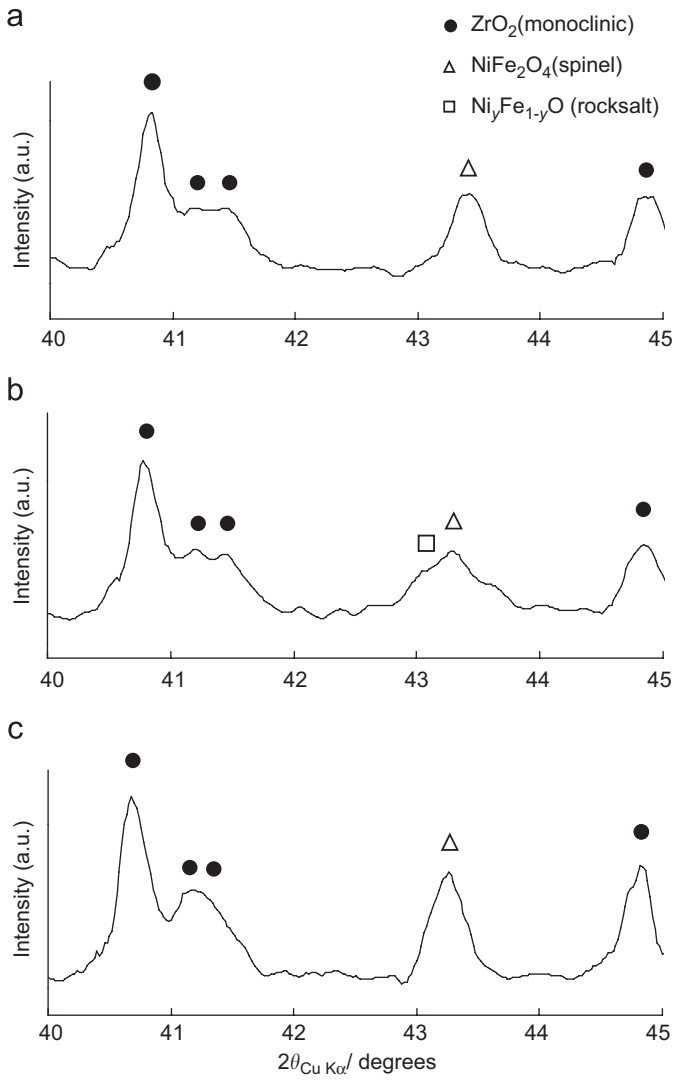

Fig. 8 – XRD patterns of the $NiFe_2O_4/ZrO_2$ samples: (a) non-treated, (b) after the T-R step in the internally circulating fluidized bed reactor and (c) after the subsequent W-D step in the fixed bed reactor.

Table 3 – Hydrogen production volume and ferrite conversion by the internally circulating $NiFe_2O_4/m$-ZrO_2 fluidized bed reactor of stainless steel

Total irradiating time (min)	Sample weight (g)	Input energy (kW)	Volume of hydrogen ($Ncm^3\,g^{-1}$ material)	Ferrite conversion (%)
15	35	1.22[a] (2297 kW/m^2)[b]	8.4	41
30	35	1.22[a] (2297 kW/m^2)[b]	9.0	44

[a] Input power of the incident Xe-beam into the reactor.
[b] Maximum energy flux density of the incident beam at the central position of the spot.

in intensity. These results indicate that the reduced phase of Ni-doped wustite was almost oxidized back to the ferrite phase.

The second test reactor made of stainless steel was tested for the T-R step of Xe-beam irradiation. The hydrogen volume and estimated ferrite conversions are given in Table 3. The volume of hydrogen produced and the ferrite conversion attained 8.4 Ncm^3 per weight of material and 41% for irradiation of 15 min. In the 2nd run, the Xe-beam irradiation was restarted and continued for another 15 min (total irradiation time 30 min). The hydrogen production and ferrite conversion were further increased to 9.0 Ncm^3 and 44%, respectively.

The change in the BET surface area of $NiFe_2O_4/m$-ZrO_2 sample shown in Table 3 was measured before and after the repeated thermal reduction without pulverization process. The surface area of the initial $NiFe_2O_4/m$-ZrO_2 sample was 10.1 $m^2\,g^{-1}$. The surface area was then reduced to 8.8 $m^2\,g^{-1}$ after the 1st run of the thermal reduction but it still remained at the same order of magnitude (5.7 $m^2\,g^{-1}$) after the 2nd run. However, in the case that $NiFe_2O_4/m$-ZrO_2 sample underwent a thermal reduction for 30 min by a fixed bed reactor, the $NiFe_2O_4/m$-ZrO_2 sample formed a porous and brittle pellet, and the BET surface area of the pulverized sample was significantly reduced to 0.4 $m^2\,g^{-1}$ after the 1st run of the repeated cycle; 0.9 $m^2\,g^{-1}$ after the 6th run [13]. This indicates that the fluidization of $NiFe_2O_4/m$-ZrO_2 during the thermal reduction of 30 min prevented the sample from sintering severely.

On the basis of the reactor concept proposed in this study, the thermal reduction by direct Xe-beam irradiation was examined for an internally circulating fluidized bed of $NiFe_2O_4/ZrO_2$ particles. As a result, the reactors enabled $NiFe_2O_4/ZrO_2$ samples to remain in powder form without sintering and agglomerating at high-temperature during the T-R step with direct irradiation for 30 min. This is an important factor in being able to continue with the subsequent W-D step in the same reactor, without the need for a pulverization process. Therefore, switching of the feed gas passing into the reactor from N_2 gas for the T-R step to steam for the W-D step is possible in a single reactor, without the need for removal, pulverization, and transfer of the reactant material to another reactor.

From the results of XRD patterns shown in Fig. 8, the thermal-reduction reaction of $NiFe_2O_4$ is written by

$$NiFe_2O_4(s) = 3Ni_yFe_{1-y}O(s) + 1/2O_2(g) \quad \Delta H_{298K} = ?? \tag{4}$$

However, the enthalpy change ΔH_{298K} of Eq. (4) is unknown and is not reported yet. Thus, the energy conversion of the reactor was estimated by following assumption that thermal-reduction reaction of $NiFe_2O_4$ proceeds at Eq. (5):

$$NiFe_2O_4(s) = NiO(s) + 2FeO(s) + 1/2O_2(g) \quad \Delta H_{298\,K} = 308.78\,kJ/mol. \tag{5}$$

In Eq. (5), a reduced phase of Ni-doped wustite ($Ni_yFe_{1-y}O$) is not formed, but pure two phases of NiO and FeO occur after thermal reduction of $NiFe_2O_4$. These points are different from the experimental results of XRD analysis (Fig. 8). As a result, under the present experimental conditions, the kinetics for thermal reduction in an internally circulating fluidized bed of $NiFe_2O_4/ZrO_2$ were too slow to yield an energy efficiency of interest ($\eta < 1\%$). The main reason for the slow kinetics is the fact that the input power for concentrated Xe-beam is only 1.2 kW and too small. Thus, the temperature of the overall bed would not reach the temperature required for thermal reduction of $NiFe_2O_4$ (>1400 °C), while only the directly irradiated part of the bed, positioned at a center and top of the bed, was thermally reduced. This problem would probably be solved using increased input power.

4. Summary

A new concept for a windowed solar chemical reactor using an internally circulating fluidized bed of ferrite/ZrO_2 particles was proposed for the thermochemical two-step water-splitting cycle. On the basis of this concept, chemical reactors made of quartz and stainless steel were tested for thermal reduction of $NiFe_2O_4/ZrO_2$ particles on a laboratory scale using solar-simulating Xe-beam direct irradiation. The chemical reactor enabled the $NiFe_2O_4/ZrO_2$ sample to remain in powder form without sintering and agglomerating during direct Xe-beam irradiation over 30 min. The BET surface area of the fluidized $NiFe_2O_4/ZrO_2$ sample, which was 10.1 $m^2\,g^{-1}$ before irradiation, remained to be 5.7 $m^2\,g^{-1}$ after the thermal reduction of 30 min. Through the direct irradiation of the fluidized $NiFe_2O_4/ZrO_2$ bed by the solar-simulated high-flux beam, approximately 45% of the $NiFe_2O_4$ was converted to the reduced phase, and was then completely reoxidized with steam at 1000 °C to generate hydrogen.

REFERENCES

[1] Kalogirou AS. Solar thermal collectors and applications. Prog Energy Combust Sci 2004;30:231–95.

[2] Mills D. Advances in solar thermal electricity technology. Sol Energy 2004;76:19–31.

[3] Johnston G, Lovegrove K, Luzzi A. Optical performance of spherical reflecting elements for use with paraboloidal dish concentrators. Sol Energy 2003;74:133–40.

[4] Nakamura T. Hydrogen production from water utilizing solar heat at high temperatures. Sol Energy 1977;19: 467–75.

[5] Kodama T. High-temperature solar chemistry for converting solar heat to chemical fuels. Prog Energy Combust Sci 2003;29:567–97.

[6] Darken LS, Gurry RW. The system iron–oxygen. II. Equilibrium and thermodynamics of liquid oxide and other phase. J Am Chem Soc 1946;63:798–816.

[7] Lundberg M. Model calculations on some feasible two-step water splitting processes. Int J Hydrogen Energy 1993;18(5):369–76.

[8] Ehrensberger K, Frei A, Kuhn P, Oswald H, Hug P. Comparative experimental investigations of the water-splitting reaction with iron oxide $Fe_{1-y}O$ and iron manganese oxides $(Fe_{1-x}Mn_x)_{1-y}O$. Solid State Ionics 1995;78: 151–60.

[9] Ehrensberger K, Kuhn P, Shklover V, Oswald H. Temporary phase segregation processes during the oxidation of $(Fe_{0.7}Mn_{0.3})_{0.99}O$ in N_2-H_2O atmosphere. Solid State Ionics 1996;90:75–81.

[10] Tamaura T, Steinfeld A, Kuhn P, Ehrensberger K. Production of solar hydrogen by a novel, 2-step, water-splitting thermochemical cycle. Energy 1995;20(4):325–30.

[11] Kodama T, Kondoh Y, Kiyama A, Shimizu K-I. Hydrogen production by solar thermochemical water-splitting/ methane-reforming process. In: Thornbloom MD, Jones SA, editors. Proceeding of ASME international solar energy conference (ISEC) 2003, Hawaii, 2003. New York: ASME; ISEC2003-44037 (CD-ROM publication).

[12] Kodama T, Kondoh Y, Yamamoto R, Andou H, Satoh N. Thermochemical hydrogen production by a redox system of ZrO_2-supported Co(II)-ferrite. Sol Energy 2005;78: 623–31.

[13] Kodama T, Gokon N, Yamamoto R. Thermochemical two-step water splitting by ZrO_2-supported $Ni_xFe_{3-x}O_4$ for solar hydrogen production, Sol Energy 2008;82:73–9.

[14] Agrafiotis C, Roeb M, Konstandopoulos AG, Nalbandian L, Zaspalis VT, Sattler C, et al. Solar water splitting for hydrogen

production with monolithic reactors. Sol Energy 2005;79:409–21.
[15] Roeb M, Sattler C, Klüser R, Monnerie N, Oliveira L, Konstandopoulos AG, et al. Solar hydrogen production by a two-step cycle based on mixed iron oxides. J Sol Energy Eng 2006;128:125–33.
[16] Haueter P, Moeller S, Palumbo R, Steinfeld A. The production of zinc by thermal dissociation of zinc oxide—solar chemical reactor design. Sol Energy 1999;67(1–3):161–7.
[17] Meier A, Ganz J, Steinfeld A. Modeling of a novel high-temperature solar chemical reactor. Chem Eng Sci 1996;51(11):3181–6.
[18] Weidenkaff A, Brack M, Möller S, Palumbo R, Steinfeld A. Solar thermal production zinc: program strategy and status of research. J Phys IV France 1999;9:Pr3-313–8.
[19] Segal A, Epstein M. The optics of the solar tower reflector. Sol Energy 2000;69(Suppl):229–41.
[20] Segal A, Epstein M. Solar ground reformer. Sol Energy 2003;75:479–90.
[21] Abe M, Tanno Y, Tamaura Y. Direct formation of ferrite film in wet process. J Appl Phys 1985;57(1):3795–7.
[22] Tamaura Y, Abe M, Itoh T. Magnetic thin film formation reaction of ferrite in aqueous solution. J Chem Soc Jpn 1987;11:1980–7.